Biochemical and Biophysical Research Communications 430 (2013) 196–201

Contents lists available at SciVerse ScienceDirect

Biochemical and Biophysical Research Communications

journal homepage: www.elsevier.com/locate/ybbrc

PRL-3 activates NF-κB signaling pathway by interacting with RAP1

Shenyi Lian [a], Lin Meng [a], Caiyun Liu [a], Xiaofang Xing [a], Qian Song [a], Bin Dong [b], Yong Han [a], Yongyong Yang [a], Lirong Peng [c], Like Qu [a], Chengchao Shou [a,*]

[a] Key Laboratory of Carcinogenesis and Translational Research (Ministry of Education), Department of Biochemistry and Molecular Biology, Peking University Cancer Hospital & Institute, Beijing 100142, China
[b] Key Laboratory of Carcinogenesis and Translational Research (Ministry of Education), Department of Pathology, Peking University Cancer Hospital & Institute, Beijing 100142, China
[c] Department of Molecular Oncology, H. Lee Moffitt Cancer Center & Research Institute, Tampa, FL 33612, United States

ARTICLE INFO

Article history:
Received 23 October 2012
Available online 21 November 2012

Keywords:
PRL-3
RAP1
NF-κB
Cancer

ABSTRACT

Phosphatase of regenerating liver (PRL-3) promotes cancer metastasis through enhanced cell motility and invasiveness, however its role in tumorigenesis remains unclear. Herein, we reported that PRL-3 interacts with telomere-related protein RAP1. PRL-3 promotes the cytosolic localization of RAP1, which is counteracted by silencing of PRL-3. Immunohistochemical staining of colon cancer tissue array ($n = 170$) revealed that high level of PRL-3 associates with cytosolic localization of RAP1 ($p = 0.01$). Microarray analysis showed that PRL-3 regulates expression of diverse genes and enhances phosphorylation of p65 subunit of NF-κB in a RAP1-dependent manner. Furthermore, PRL-3 transcriptionally activates RAP1 expression, which is counteracted by ablating p65. Therefore, our results demonstrate PRL-3 as a novel regulator of NF-κB signaling pathway through RAP1.

1. Introduction

The protein tyrosine phosphatases (PTPs) constitute a superfamily of enzymes serving as the critical regulatory components in signal transduction pathways [1]. The phosphatase of regenerating liver (PRL) family of PTPs, including PRL-1, PRL-2, and PRL-3, emerges as potential biomarkers and therapeutic targets for various types of malignancy [2–4]. PRL-3 is frequently overexpressed in a variety of cancer tissues, which correlates with disease progression and patients' survival [5–8]. Mutation at PRL-3's catalytic domain could reduce cancer cell motility, suggesting PRL-3's PTP activity is essential for cancer cell migration [9,10]. Mechanistic investigations show that PRL-3 stimulates invasion and motility of cancer cells by activating the Rho family of small GTPases and the matrix metalloproteinase-2 (MMP-2) [11,12]. PRL-3 negatively regulates C-terminal Src kinase (Csk) and PTEN, leading to enhanced activities of Src kinase and PI3K/AKT signaling pathways [13–15]. By upregulating the activity of STAT (signal transducers and activators of transcription) pathway and the expression of anti-apoptotic factor Mcl-1, PRL-3 confers therapeutic resistance to small molecule inhibitors [16]. Additionally, PRL-3 could enhance ubiquitination and proteasome-mediated degradation of tumor suppressor p53 [17,18]. Despite of these findings, the role of PRL-3 in tumorigenesis remains elusive.

RAP1 (Repressor/Activator Protein 1; or TRF2IP1, Telomeric Repeat Binding Factor 2 Interacting Protein 1) was initially identified from *Saccharomyces cerevisiae*, which is not only required for safeguarding chromosome ends to ensure chromosomal stability, but also has unique functions in other contexts [19,20]. Ectopic expression of human RAP1 was shown to accelerate telomere lengthening [21]. By gene knockout approach, RAP1 was shown to be essential for repressing homology-directed repair (HDR) and inhibiting telomeric sister chromatid exchanges (T-SCEs) [22]. By chromatin immunoprecipitation (ChIP)-coupled with high-throughput sequencing, RAP1 was found to bind non-telomere DNA sequences, which may modulate gene expression [23]. In the cytoplasma, RAP1 forms a complex with IκB kinases (IKKs) and promotes IKKs-mediated phosphorylation of the p65 subunit of NF-κB. Knock down of RAP1 impairs the NF-κB signal cascade through decreased interaction between IKK1/2 and p65. RAP1-mutant mice are resistant to endotoxic response and are defected in NF-κB signal pathway upon lipopolysaccharide treatment. NF-κB also transcriptionally activates RAP1, indicating a feedback regulation of RAP1 and NF-κB pathway [24].

In this study, we identified RAP1 as novel PRL-3-binding protein. PRL-3 promotes the cytosolic localization of RAP1. PRL-3 regulates expression of diverse genes and enhances phosphorylation of p65 in a RAP1-dependent manner. Moreover, PRL-3 activates RAP1 expression, which is abolished by silencing of p65. Therefore, PRL-3 functions as a regulator of NF-κB signaling pathway through RAP1.

Abbreviations: PRL-3, phosphatase of regenerating liver-3; RAP1, repressor/activator protein 1; PTP, protein tyrosine phosphatases.

* Corresponding author. Address: 52 Fucheng Road, Beijing 100142, China. Fax: +86 10 88122437.
E-mail address: scc@bjcancer.org (C. Shou).

0006-291X/$ - see front matter © 2012 Elsevier Inc. All rights reserved.
http://dx.doi.org/10.1016/j.bbrc.2012.11.036

2. Materials and methods

2.1. Cell lines and antibodies

The human colon cancer cell lines HCT116 and LoVo were maintained in Dulbecco's modified eagle medium (DMEM, Invitrogen). Gastric cancer cell lines BGC823, MGC 803, AGS, 7901, N87, colon cancer cell lines SW480, CL187, HT29, RKO, lung cancer cell lines PG, GLC82, H446, H460, H1299 and A549 were grown in RPMI-1640 medium (Invitrogen, Carlsbad, CA). The media were supplemented with 10% heat-inactivated fetal bovine serum (FBS, Invitrogen) plus antibiotics.

Mouse anti-PRL-3 (clone 318, SC-130355), rabbit anti-p65 (SC-372), and rabbit anti-β-tubulin (SC-9104) were purchased from Santa Cruz (Santa Cruz, CA). Rabbit anti-RAP1 (A300-306A-2) was from obtained from Bethyl (Montgomery, TX). Rabbit anti-GAPDH (10494-1-AP) was from Proteintech (Chicago, IL). Rabbit anti-Histone 2B (H2B, Ab18977) was from Abcam (Cambridge, MA). Rabbit anti-phosph-p65 (serine536, 3031S) was from Cell signaling (Danvers, MA).FITC-conjugated anti-rabbit secondary antibody (ZF-0311) was from ZSGB-Bio (Beijing, China). Rabbit anti-myc tag (AB103) and anti-GST tag (AB101) were from TianGen Biotech (Beijing, China).

2.2. Transfection, stable cell line generation and RNA interference

Full-length human RAP1 and PRL-3 cDNAs were cloned from a cDNA library of colon cancer cell and verified by sequencing. PRL-3 cDNA was inserted into the pcDNA3 vector. To generate cell line stably expressing PRL-3 and control cell line (HCT116-PRL-3 and HCT116 con), HCT116 cells were transfected with pcDNA3-myc-PRL-3 or pcDNA3 using Lipofectamine 2000 reagent (Invitrogen) following provider's suggestion. Cells were selected with 400 μg/ml of G418 (Sigma, St. Louis, MO) for 3 weeks, and resistant colonies were pooled for subsequent studies. The sequence of RAP1-specific short hairpin RNA (shRNA) is 5′-CACCGGAGGATTG AATTTCGAAAGATTCAAGAGATCTTTCGAAATTCAATCCTCCTTTTTTG-3′. The control shRNA sequcence is 5′-CCTAAGGTTAAGTCGCCCTCG CTCGAGCGAGGGCGACTTAACCTTAGG-3′. PRL-3-specific small interference RNA (siRNA) sequences are 5′-CTTCCTCATCACCCAC AACC-3′ (PRL-3-1) and 5′-CAGCAAGCAGCTCACCTAC-3′ (PRL-3-2). P65-specific siRNA sequence is 5′-CAUAUGAGACCUUCAAGAGC A-3′. The control siRNA sequence is 5′- AATTCTCCGAACGTGTCAC G-3'. The shRNAs and siRNAs were synthesized by GenePharma (Shanghai, China) and transfected into cells with Lipofectamine 2000 reagent.

2.3. GST pull-down assay

GST-tagged RAP1 was constructed by inserting RAP1 cDNA into pGEX-4T1 vector. His-tagged PRL-3 was constructed by inserting the PRL-3 cDNA into pET-28a vector. For pull-down assay, glutathione-Sepharose beads (Invitrogen) were incubated with GST-RAP1 or GST purified from E. coli bacteria. After washed with phosphate-buffered saline (PBS), these beads were incubated with purified His-PRL-3 in binding buffer (10 mM Tris–HCl pH 8.0, 150 mM NaCl, 1 mM dithiothreitol, 1 mM PMSF, 1% Triton-100, 10% glycerol) for 4 h at 4 °C. The precipitates were washed three times, boiled in 2x Laemmli loading buffer, separated by SDS–PAGE, and immunoblotted with an anti-PRL-3 antibody.

2.4. Western blotting and immunoprecipitation

Cells were directly homogenized in 2x Laemmli loading buffer for Western analysis. Equal loading was verified by probing with anti-GAPDH. Alternatively, to make cytosolic and nuclear extracts, cells at 80% confluence were homogenized in ice-cold buffer A (10 mM HEPES pH 7.9, 10 mM KCl, 0.1 mM EDTA, 1 mM DTT, and 1x protease inhibitor cocktail (Roche, Indianapolis, IN)) on ice for 20 min. Samples were then supplemented with NP-40 to 0.5% (v/v), vortexed, incubated for another 10 min, and centrifuged at 1500g for 5 min at 4 °C. The supernatants were recovered to obtain the cytosolic extracts. The pellets (nuclei) were washed twice with ice-cold buffer A and directly homogenized in 2x loading buffer to obtain the nuclear extract. The purities of cytosolic and nuclear extracts were respectively verified by probing with anti-β-tubulin and anti-H2B. For immunoprecipitation assay, cells were homogenized in ice-cold lysis buffer containing 50 mM Tris–HCl pH 7.4, 300 mM NaCl, 50 mM NaF, 1 mM EDTA, 1 mM DTT, 1% Triton X-100, 10% glycerol, and 1x protease inhibitor cocktail. After 20 min incubation on ice, the samples were centrifuged at 12,000 rpm for 15 min, and the supernatant was recovered. After being pre-cleared with protein A/G-coupled Sepharose beads (Invitrogen) for 2 h, the cell lysates were immunoprecipitated with anti-RAP1 antibody plus protein A/G Sepharose for 8 h at 4 °C. Pre-immune serum was used as control. The precipitates were washed four times with lysis buffer, once with ice-cold PBS, and boiled in 2x loading buffer. Protein samples were resolved by SDS–PAGE and electroblotted onto nitrocellulose membranes, which were blocked in 5% skim milk in PBST and probed with the indicated antibodies. Protein bands were visualized with enhanced chemoluminescence system (Thermo Scientific, Rockford, IL).

2.5. Immunofluorescence (IF) staining

Cells were grown on coverslips to 60% confluence, and fixed with cold methanol/acetic acid (1:1). Next, cells were permeabilized with 0.5% Triton X-100 in PBS, washed with PBS, blocked with 5% goat serum (Sigma) at room temperature for 1 h, and incubated with anti-RAP1 antibody at 4 °C for 16 h. After washing with 0.1% Tween 20 in PBS for 5 times, cells were incubated with FITC-conjugated secondary antibody at room temperature for 45 min, followed by washing with 0.1% Tween 20 in PBS, and counterstaining with 4′,6-diamidino-2-phenylindole (DAPI). Images were acquired using a Leica TCS SP5 laser confocal microscope with identical setting at room temperature.

2.6. Tissue microarray immunohistochemistry

Tumor-specific tissue microarray (TMAs, BC051111, Chaoyang Bio, Shaanxi, China) is paraffin-embedded block containing 170 unique cases of colon adenocarcinoma with varying grade and diagnosis. A pair of slides were dewaxed, rehydrated through gradient alcohol, followed by heat-induced antigen retrieval using EDTA-based retrieval solution for 20 min at 100 °C. Endogenous peroxidase was blocked by H_2O_2 and background was blocked with 5% nonfat milk in PBS. TMAs were then incubated with anti-RAP1 or anti-PRL-3 antibodies overnight at 4 °C. After washing with PBS, TMAs were probed with EnVision (Dako Cytomation, Carpinteria, CA) at room temperature for 45 min. The stained TMAs were independently evaluated by two pathologists. The expressions of PRL-3 and RAP1 were evaluated by two pathologists independently according to the previous studies [8,24].

2.7. Microarray analysis and quantitative RT-PCR

RNA was extracted from cells with Trizol reagent (Invitrogen). Gene expression profiles in HCT116-PRL-3 and HCT116 con cells were examined using Affymetrix GeneChip containing 41,000 transcripts and variants. After normalization, the fold change of gene expression was calculated. A P value less than 0.05 and the

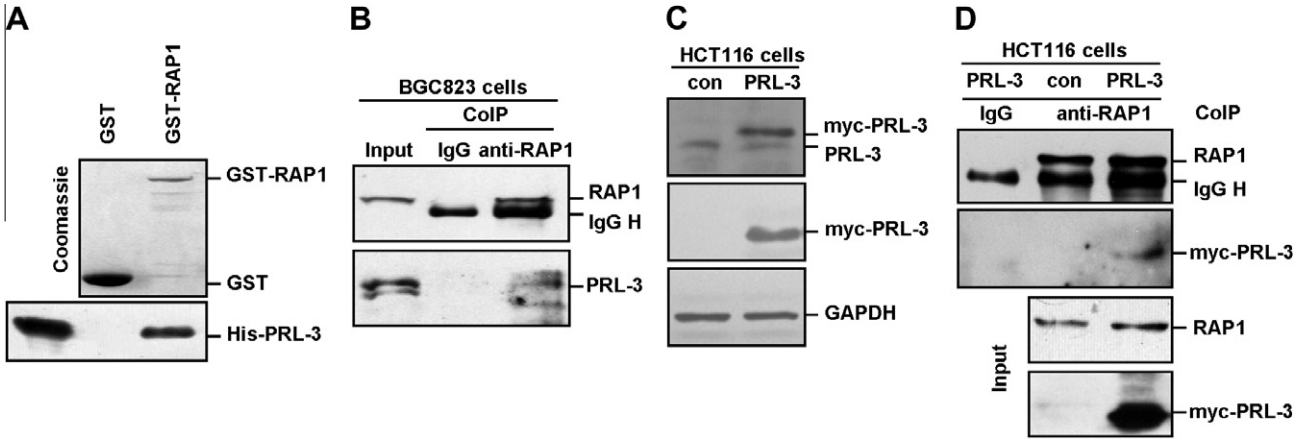

Fig. 1. PRL-3 interacts with RAP1 and promotes cytosolic localization of RAP1. (A) In vitro interaction between PRL-3 and RAP1. Recombinant His-PRL-3 and GST-RAP1 proteins were bacterially expressed, purified, and analyzed by in vitro pull-down assays. GST fusion proteins were shown by Coomassie blue staining. Precipitated His-PRL-3 was detected by Western blot with antibody against PRL-3. (B) Endogenous protein–protein interactions. Protein lysates (500 μg) from BGC823 cells were immunoprecipitated with a polyclonal anti-RAP1 antibody or preimmune rabbit serum (as control). Precipitates and 100 μg protein (as input) were analyzed by Western blot with indicated antibodies. IgG H, IgG heavy chain. (C) Stable expression of myc-PRL-3 in HCT116 cells. Pooled colonies were collected and protein lysates were subjected to Western blot with indicated antibodies. (D) Association between endogenous RAP1 and exogenous PRL-3. Protein lysates from indicated cells were immunoprecipitated with a polyclonal anti-RAP1 antibody, followed by Western blot with antibodies against myc-tag and RAP1.

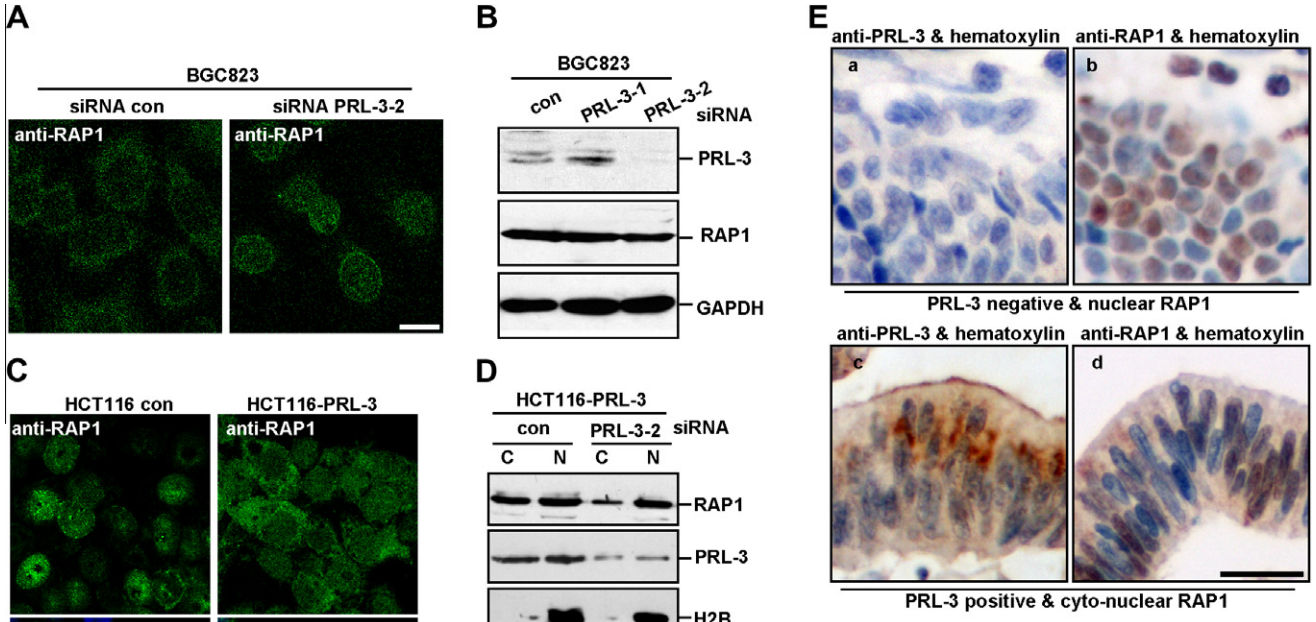

F Correlation between PRL-3 and cytosolic RAP1 in colon cancer tissues

Cyto RAP1	PRL-3 Negative	PRL-3 Positive	Total	*P* value
Negative	104	24	128	0.010
Positive	26	16	42	
Total	130	40	170	

Fig. 2. PRL-3 promotes the cytosolic localization of RAP1. (A) Localization of RAP1 in BGC823 cells. Cells were transfected with 50 nM indicated siRNAs for 48 h, followed by staining with anti-RAP1 (green). Nuclei were counterstained with DAPI (blue). Scale bar, 10 μm. (B) Verification of the silencing efficiency of siRNAs against PRL-3. 50 nM indicated siRNAs were transfected into BGC823 cells for 48 h. (C) Immunostaining of RAP1 (green) in HCT116 cells. Nuclei were counterstained with DAPI (blue). Scale bar, 10 μm. (D) Knock-down of ectopic PRL-3 decreased cytosolic distribution of RAP1. HCT116-PRL-3 cells were transfected with 50 nM indicated siRNAs for 48 h, and the cytosolic (C) and nuclear (N) lysates were analyzed by Western blot. Anti-β-tubulin and anti-H2B were used to monitor the purities of cytosolic and nuclear lysates, respectively. (E) Immunohistochemical staining of PRL-3 and RAP1 in colon adenocarcinoma tissue arrays. Representative images of two pairs of consecutive sections were shown. a, negative PRL-3 staining; b, nuclear RAP1 staining; c, positive PRL-3 staining; d, nuclear and cytosolic RAP1 staining. X40 magnification; Scale bar, 100 μm. and (F) Correlation between PRL-3 and cytosolic RAP1 in colon adenocarcinoma tissues ($n = 170$). P value was calculated by chi-squared test using SPSS software.

fold-change threshold 2 were chosen as significant alterations in transcription. The differentially expressed genes were analyzed by MeV software (Designed by Dana-Farber Cancer Institute). For validation of the expression profiles, quantitative RT-PCR reactions were performed using SYBR Green (Applied Biosystem) according to manufacturer's instructions. mRNA level of *GAPDH* was used

as internal control. Setting for amplification was 95 °C for 30 s, followed by 40 cycles of 95 °C for 30 s, 60 °C for 30 s, and 72 °C for 30 s. Primer sequences were shown in Supplemental Table S1.

2.8. Statistical analysis

Statistical significance was calculated by two-tailed Student's *t* test or chi-squared test using SPSS (IBM, Version19.0) software.

3. Results

3.1. PRL-3 interacts with RAP1

To further elucidate mechanism underlying the role of PRL-3 in tumorigenesis, yeast two-hybrid screening was performed with the full length human PRL-3 cDNA as bait. We identified RAP1 as a novel PRL-3 interacting protein. A direct interaction between PRL-3 and RAP1 was confirmed by GST pull-down assay using purified recombinant proteins (Fig. 1A). Co-immunoprecipitation assay with protein lysates from BGC823 gastric cancer cells revealed the association between endogenous PRL-3 and RAP1 (Fig. 1B). Next, we stably expressed exogenous PRL-3 in the HCT116 colon cancer cells (Fig 1C). The endogenous RAP1 could also interact with exogenous PRL-3 in the co-immunoprecipitation assay (Fig. 1D).

3.2. PRL-3 promotes the cytosolic localization of RAP1

Although RAP1 was regarded as a nuclear protein, recent study highlighted the critical role of cytosolic RAP1 in NF-κB signaling [24]. However, factor(s) determining the cytosolic localization of RAP1 is unclear. Considering the interaction between PRL-3 and RAP1, we sought to investigate the effect of PRL-3 on RAP1's localization. Immunofluorescent staining of BGC823 cells revealed that RAP1 was mainly localized in the cytoplasma (Fig. 2A). By efficiently silencing endogenous PRL-3 with a siRNA (PRL-3-2) (Fig. 2B), the cytosolic level of RAP1 was decreased and the nuclear abundance of RAP1 was increased (Fig. 2A). Unlike in BGC823 cells, RAP1 predominantly exhibited nuclear staining in HCT116 con

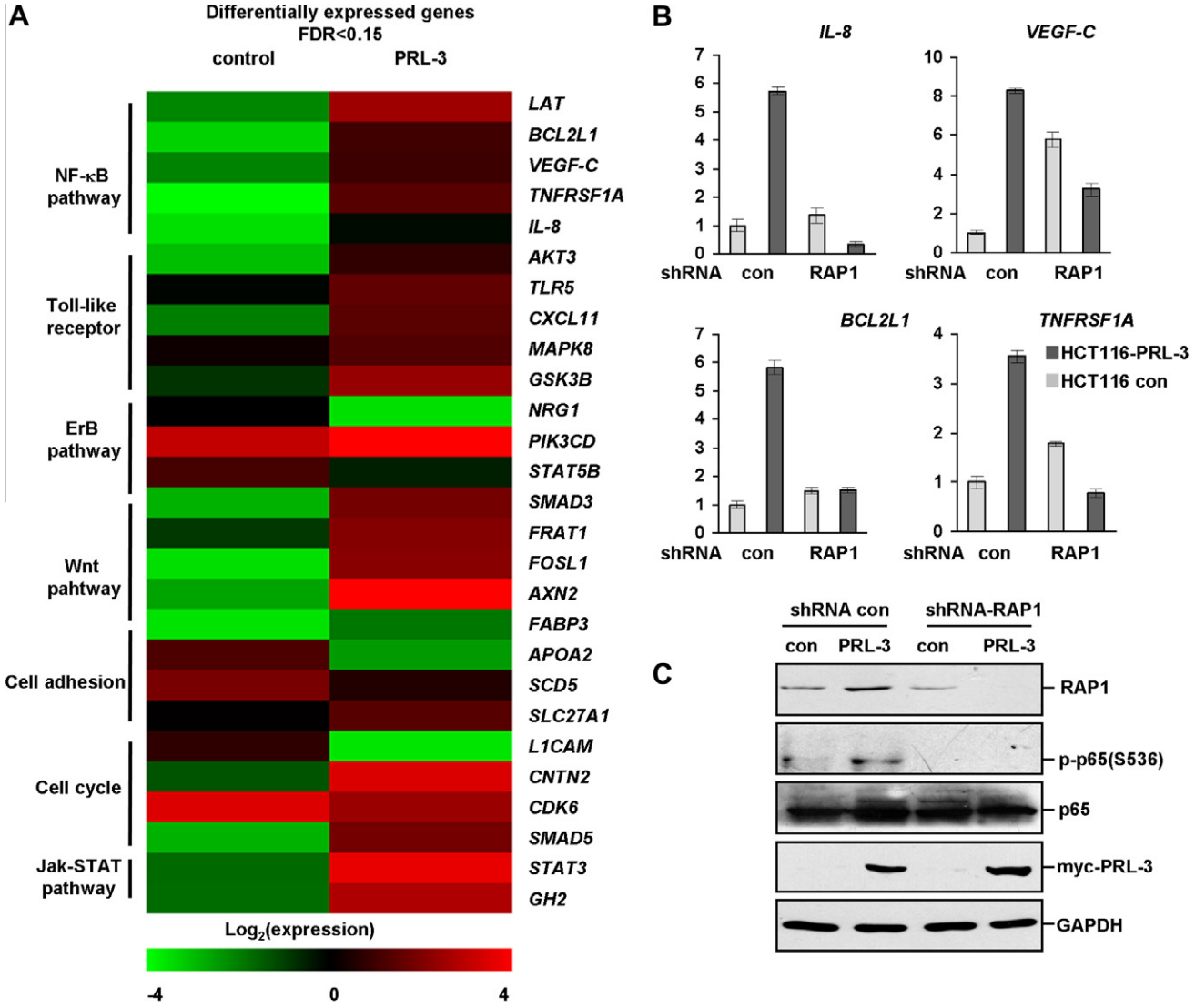

Fig. 3. PRL-3 activates NF-κB signaling pathway. (A) Differentially expressed genes affected by PRL-3 in HCT116 cells. The color intensity is proportional to the $\log_2$ of expression ratio (green, downregulated; red, upregulated). Biological processes are listed on the left. All genes had a FDR (False Discovery Rate) <0.15. (B) RAP1 contributes to PRL-3-regulated gene expression. Cells were transfected with indicated shRNAs for 72 h, and RNA samples were subjected to quantitative RT-PCR analysis with primers for indicated genes. Data show mean values ± SD from two independent experiments. (C) RAP1 contributes to PRL-3-promoted p65 phosphorylation. Cells were transfected as in (B), and cell lysates were analyzed by Western blotting.

cells, but cytosolic distribution of RAP1 was found in the majority of HCT116-PRL-3 cells (Fig. 2C). Next, subcellular fractionation assay confirmed RAP1's cytosolic expression in HCT116-PRL-3 cells (Fig. 2D). By knocking down ectopic PRL-3 with siRNA, cytosolic level of RAP1 was decreased (Fig. 2D). To substantiate above results, a pair of colon adenocarcinoma tissue microarrays were immunostained with antibodies against PRL-3 and RAP1, respectively (Fig. 2E). We found there was higher incidence of cytosolic RAP1 in samples with positive PRL-3 than in those with negative PRL-3 expression ($P = 0.01$) (Fig. 2F). Therefore, PRL-3 is capable of inducing cytosolic localization of RAP1.

3.3. RAP1 contributes to PRL-3-regulated gene expression and phosphorylation of p65

With RNA samples extracted from HCT116 con and HCT116-PRL-3 cells, microarray analysis was performed to examine PRL-3's effect on gene expression profiles. Expression of 2697 genes was found to be altered by PRL-3, including 1394 upregulated and 1303 downregulated genes (profiles of representative genes were shown in Fig. 3A). These genes participate in pathways related to diverse aspects of physiological and pathological processes, such as Toll-like receptor, ErbB, Wnt, PPAR, and NF-κB pathways. We chose some of NF-κB pathway-related genes and confirmed higher *IL-8*, *VEGF-C*, *BCL2L1* and *TNFSF1A* expression in HCT116-PRL-3 cells than in HCT116 con cells by quantitative RT-PCR (Fig. 3B), indicating PRL-3 activates NF-κB signaling. In line with these results, we observed enhanced phosphorylation of p65 in HCT116-PRL-3 cells (Fig. 3C). Considering the regulatory role of RAP1 in NF-κB pathway [24], we evaluated RAP1's effect on PRL-3-regulated gene expression. To this end, RAP1 was silenced by shRNA (Fig. 3C). Following this treatment, both PRL-3-stimulated gene up-regulation and p65 phosphorylation were greatly impaired (Fig. 3B and C). These results show that RAP1 is essential for PRL-3-regulated gene expression and phosphorylation of p65.

3.4. PRL-3 promotes RAP1 expression through p65

We found there was more RAP1 expression in HCT116-PRL-3 cells than in control cells (Figs. 1D and 3C), and silencing of endogenous PRL-3 resulted in decreased RAP1 protein in BGC823 cells (Fig. 2B). Result of quantitative RT-PCR analysis showed higher mRNA expression of RAP1 in HCT116-PRL-3 cells (Fig. 4A). By examining RNA samples from 17 cancer cell lines, we found mRNA levels of RAP1 tended to be higher in cells expressing more PRL-3 (Fig. 4B). Since NF-κB could activate transcription of RAP1 [24] and PRL-3 stimulates NF-κB in a RAP1-dependent manner (this study), we then knocked down p65 by siRNA. After ablation of p65, PRL-3-promoted RAP1 was diminished (Fig. 4C). Thus, PRL-3 promotes RAP1 expression through p65.

4. Discussion

In this study, we identified a physical interaction between PRL-3 and telomere-binding protein RAP1. RAP1 mainly resides in the nucleus and partially in the cytoplasma [23,24], however the precise mechanism controlling RAP1 shuttles between nucleus and cytoplasma is unclear. Despite the localization of RAP1 is distinct in BGC823 cells and in HCT116 cells, we found cytosolic levels of RAP1 could be modulated by silencing or overexpression of PRL-3. Supported by TMA analysis, our results suggest a regulatory role of PRL-3 in determining the subcellular localization of RAP1.

Through differential gene expression screening, we found PRL-3 affects expression of diverse genes, which are categorized into distinct pathways. The profiling results are not only complement with

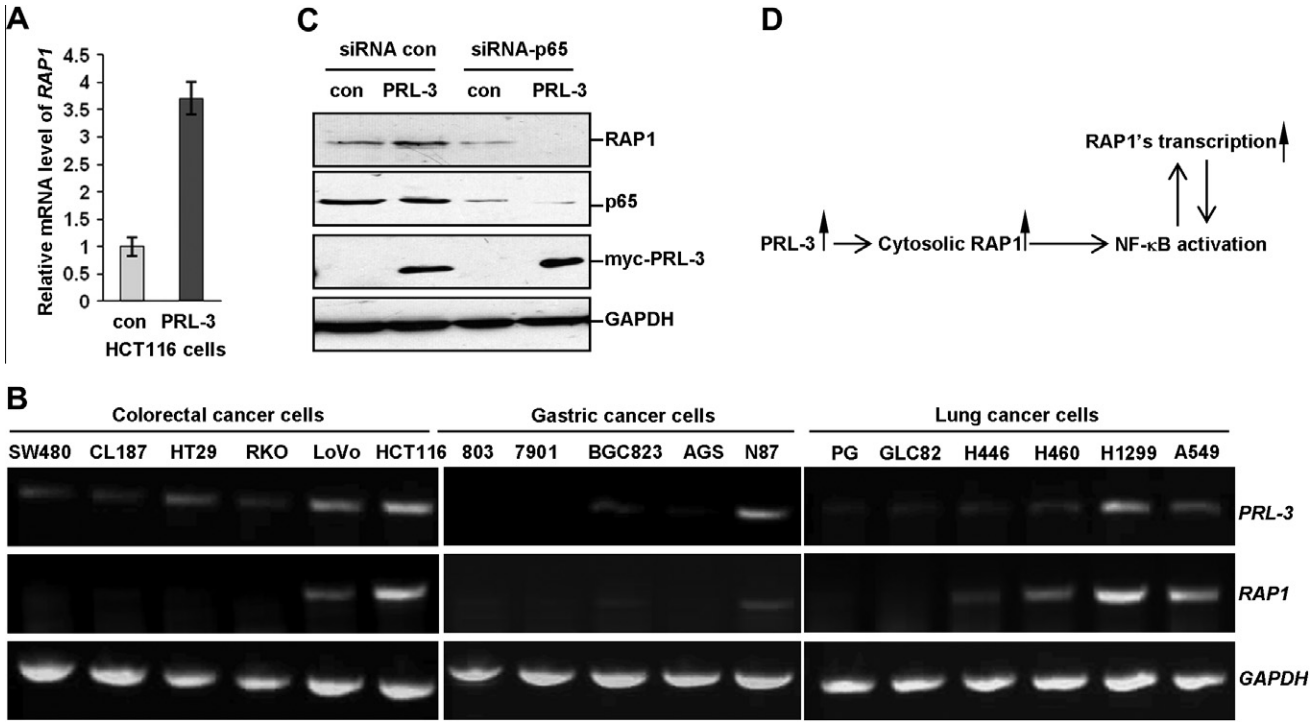

Fig. 4. PRL-3 promotes RAP1 expression through p65. (A) Quantitative RT-PCR analysis of RAP1 expression in HCT116 con and HCT116-PRL-3 cells. Data show mean values ± SD from two independent experiments. (B) RT-PCR analysis of PRL-3 and RAP1 expression in different cancer cell lines. (C) PRL-3 increases RAP1 protein level in a p65-dependent manner. HCT116 cells were transfected with control or p65-specific siRNA for 72 h, and protein lysates were analyzed by Western blotting. (D) Schematic illustration of the role of PRL-3 in regulating RAP1 and NF-κB signaling. High expression of PRL-3 induces the cytosolic localization of RAP1. Subsequently, RAP1 activates the NF-κB signaling pathway, which in turn stimulates RAP1 expression.

reported function of PRL-3 in controlling cell motility, adhesion, cell cycle, and angiogenesis [2,10–12,18,25,26], but also suggest previously unrecognized roles of PRL-3. From this perspective, PRL-3 may be involved in broader context of cellular events and signaling pathways critical for tumorigenesis. We further found that PRL-3 promotes phosphorylation of p65 and regulates expression of a subset of NF-κB targets in a RAP1-dependent manner. Furthermore, we found PRL-3 activates RAP1 transcription in a p65-dependent manner. By functioning as an IKK adaptor protein, cytosolic RAP1 was shown to be essential for NF-κB cascade, meanwhile NF-κB is a positive regulator of RAP1 mRNA expression, thus forming a feedback loop [24]. Our results are in agreement with this finding, and underscore PRL-3's role in modulating RAP1-NF-κB loop via increased cytosolic RAP1 (Fig. 4D). NF-κB is pivotal for immune response and inflammation, and deregulated NF-κB has been implicated in promoting inflammation-related tumorigenesis [27–29]. Because of higher expression of PRL-3 in variety of tumors, it would be interesting to evaluate PRL-3's contribution to NF-κB signaling and to other newly characterized pathways in future investigations.

By tightly associating with TRF2 (telomere repeat factor 2), nuclear RAP1 is tethered to the chromosomal ends and plays a role in maintaining telomere homeostasis and genomic integrity [21–23,30]. Our present study focused on PRL-3-induced cytosolic localization of RAP1 and the resultant changes in gene expression, whether or not PRL-3 regulates genomic stability through RAP1 may warrant further studies.

Acknowledgments

We appreciate colleagues in Dr. Shou's lab for critical reading of the manuscript. This study was supported by the National 973 Program of China (2009CB521805) and National Natural Science Foundation of China (81230046 and 30973407).

Appendix A. Supplementary data

Supplementary data associated with this article can be found, in the online version, at http://dx.doi.org/10.1016/j.bbrc.2012.11.036.

References

[1] N.K. Tonks, Protein tyrosine phosphatases: from genes, to function, to disease, Nat. Rev. Mol. Biol. 7 (2006) 833–846.
[2] Q. Zeng, J.M. Dong, K. Guo, J. Li, H.X. Tan, V. Koh, C.J. Pallen, E. Manser, W. Hong, PRL-3 and PRL-1 promote cell migration, invasion, and metastasis, Cancer Res. 63 (2003) 2716–2722.
[3] J. Li, K. Guo, V.W. Koh, J.P. Tang, B.Q. Gan, H. Shi, H.X. Li, Q. Zeng, Generation of PRL-3- and PRL-1-specific monoclonal antibodies as potential diagnostic markers for cancer metastases, Clin. Cancer Res. 11 (2005) 2195–2204.
[4] B.J. Stephens, H. Han, V. Gokhale, D.D. Von Hoff, PRL phosphatases as potential molecular targets in cancer, Mol. Cancer Ther. 4 (2005) 1653–1661.
[5] S. Saha, A. Bardelli, P. Buckhaults, V.E. Velculescu, C. Rago, C.B. St, K.E. Romans, M.A. Choti, C. Lengauer, K.W. Kinzler, B. Vogelstein, A phosphatase associated with metastasis of colorectal cancer, Science 294 (2001) 1343–1346.
[6] L. Peng, J. Ning, L. Meng, C. Shou, The association of the expression level of protein tyrosine phosphatase PRL-3 protein with liver metastasis and prognosis of patients with colorectal cancer, J. Cancer Res. Clin. Oncol. 130 (2004) 521–526.
[7] Z. Li, W. Zhan, Z. Wang, B. Zhu, Y. He, J. Peng, S. Cai, J. Ma, Inhibition of PRL-3 gene expression in gastric cancer cell line SGC7901 via microRNA suppressed reduces peritoneal metastasis, Biochem. Biophys. Res. Commun. 348 (2006) 229–237.
[8] X. Xing, L. Peng, L. Qu, T. Ren, B. Dong, X. Su, C. Shou, Prognostic value of PRL-3 overexpression in early stages of colonic cancer, Histopathology 54 (2009) 309–318.
[9] K. Guo, J. Li, J.P. Tang, V. Koh, B.Q. Gan, Q. Zeng, Catalytic domain of PRL-3 plays an essential role in tumor metastasis: formation of PRL-3 tumors inside the blood vessels, Cancer. Biol. Ther. 3 (2004) 945–951.
[10] R. Song, F. Qian, Y.P. Li, X. Sheng, S.X. Cao, Q. Xu, Phosphatase of regenerating liver-3 localizes to cyto-membrane and is required for B16F1 melanoma cell metastasis in vitro and in vivo, PLoS One 4 (2009) e4450.
[11] J.J. Fiordalisi, P.J. Keller, A.D. Cox, PRL tyrosine phosphatases regulate rho family GTPases to promote invasion and motility, Cancer Res. 66 (2006) 3153–3161.
[12] L. Peng, X. Xing, W. Li, L. Qu, L. Meng, S. Lian, B. Jiang, J. Wu, C. Shou, PRL-3 promotes the motility, invasion, and metastasis of LoVo colon cancer cells through PRL-3-integrin beta1-ERK1/2 and-MMP2 signaling, Mol. Cancer 8 (2009) 110–122.
[13] F. Liang, Y. Luo, Y. Dong, C.D. Walls, J. Liang, H.Y. Jiang, J.R. Sanford, R.C. Wek, Z.Y. Zhang, Translational control of C-terminal Src kinase (Csk) expression by PRL3 phosphatase, J. Biol. Chem. 283 (2008) 10339–10346.
[14] H. Wang, S.Y. Quah, J.M. Dong, E. Manser, J.P. Tang, Q. Zeng, PRL3 down regulates PTEN expression and signals through PI3K promote epithelial–mesenchymal transition, Cancer Res. 67 (2007) 2922–2926.
[15] H. Lempiainen, T.D. Halazonetis, Emerging common themes in regulation of PIKKs and PI3Ks, EMBO J. 28 (2009) 3067–3073.
[16] J. Zhou, C. Bi, W.J. Chng, L.L. Cheong, S.C. Liu, S. Mahara, K.G. Tay, Q. Zeng, J. Li, K. Guo, C.P. Tan, H. Yu, D.H. Albert, C.S. Chen, PRL-3, a metastasis associated tyrosine phosphatase, is involved in FLT3-ITD signaling and implicated in anti-AML therapy, PLoS One 6 (2011) e19798.
[17] S.H. Min, D.M. Kim, Y.S. Heo, H.M. Kim, I.C. Kim, O.J. Yoo, Downregulation of p53 by phosphatase of regenerating liver 3 is mediated by MDM2 and PIRH2, Life Sci. 86 (2010) 66–72.
[18] S. Basak, S.B. Jacobs, A.J. Krieg, N. Pathak, Q. Zeng, P. Kaldis, A.J. Giaccia, L.D. Attardi, The metastasis-associated gene Prl-3 is a p53 target involved in cell-cycle regulation, Mol. Cell 30 (2008) 303–314.
[19] T. de Lange, Shelterin: the protein complex that shapes and safeguards human telomeres, Genes Dev. 19 (2005) 2100–2110.
[20] B. Li, S. Oestreich, T. de Lange, Identification of human Rap1: implications for telomere evolution, Cell 101 (2000) 471–483.
[21] M.S. O'Connor, A. Safari, D. Liu, J. Qin, S. Zhou, The human Rap1 protein complex and modulation of telomere length, J. Biol. Chem. 279 (2004) 28585–28591.
[22] A. Sfeir, S. Kabir, M. van Overbeek, G.B. Celli, T. de Lange, Loss of Rap1 induces telomere recombination in the absence of NHEJ or a DNA damage signal, Science 327 (2010) 1657–1661.
[23] P. Martinez, M. Thanasoula, A.R. Carlos, G. Gomez-Lopez, A.M. Tejera, S. Schoeftner, O. Dominguez, D.G. Pisano, M. Tarsounas, M.A. Blasco, Mammalian Rap1 controls telomere function and gene expression through binding to telomeric and extratelomeric sites, Nat. Cell Biol. 12 (2010) 768–780.
[24] H. Teo, S. Ghosh, H. Luesch, A. Ghosh, E.T. Wong, N. Malik, A. Orth, P. de Jesus, A.S. Perry, J.D. Oliver, N.L. Tran, L.J. Speiser, M. Wong, E. Saez, P. Schultz, S.K. Chanda, I.M. Verma, V. Tergaonkar, Telomere-independent Rap1 is an IKK adaptor and regulates NF-kappaB-dependent gene expression, Nat. Cell Biol. 12 (2010) 758–767.
[25] K. Guo, J. Li, H. Wang, M. Osato, J.P. Tang, S.Y. Quah, B.Q. Gan, Q. Zeng, PRL-3 initiates tumor angiogenesis by recruiting endothelial cells in vitro and in vivo, Cancer Res. 66 (2006) 9625–9635.
[26] U.M. Fagerli, R.U. Holt, T. Holien, T.K. Vaatsveen, F. Zhan, K.W. Egeberg, B. Barlogie, A. Waage, H. Aarset, H.Y. Dai, J.J. Shaughnessy, A. Sundan, M. Borset, Overexpression and involvement in migration by the metastasis-associated phosphatase PRL-3 in human myeloma cells, Blood 111 (2008) 806–815.
[27] M. Karin, F.R. Greten, NF-κB: linking inflammation and immunity to cancer development and progression, Nat. Rev. Immunol. 5 (2005) 749–759.
[28] W.E. Naugler, M. Karin, NF-κB and cancer – identifying targets and mechanisms, Curr. Opin. Genet. Dev. 18 (2008) 19–26.
[29] Y. Yamamoto, R.B. Gaynor, Therapeutic potential of inhibition of the NF-κB pathway in the treatment of inflammation and cancer, J. Clin. Invest. 107 (2001) 135–142.
[30] N.S. Bae, P. Baumann, A RAP1/TRF2 complex inhibits nonhomologous end-joining at human telomeric DNA ends, Mol. Cell 26 (2007) 323–334.